

Stochastic Electron Acceleration in Shell-Type Supernova Remnants II

Siming Liu*, Zhong-Hui Fan[†] and Christopher L. Fryer*

*Los Alamos National Laboratory, Los Alamos, NM 87545

[†]Department of Physics, Yunnan University, Kunming 650091, Yunnan, China; zhfan@ihep.ac.cn

Abstract. We discuss the generic characteristics of stochastic particle acceleration by a fully developed turbulence spectrum and show that resonant interactions of particles with high speed waves dominate the acceleration process. To produce the relativistic electrons inferred from the broadband spectrum of a few well-observed shell-type supernova remnants in the leptonic scenario for the TeV emission, fast mode waves must be excited effectively in the downstream and dominate the turbulence in the subsonic phase. Strong collisionless non-relativistic astrophysical shocks are studied with the assumption of a constant Aflvén speed. The energy density of non-thermal electrons is found to be comparable to that of the magnetic field. With reasonable parameters, the model explains observations of shell-type supernova remnants. More detailed studies are warranted to better understand the nature of supernova shocks.

Keywords: acceleration of particles — MHD — plasmas — shock waves — turbulence

PACS: 98.38.Mz

TURBULENCE CASCADE AND STOCHASTIC PARTICLE ACCELERATION

In the Kolmogorov phenomenology, the free energy dissipation rate is given by $Q \equiv C_1 \rho u^3 / L$, where C_1 is a dimensionless constant, and u and L are the eddy speed and the turbulence generation scale, respectively. The eddy turnover speed and time at smaller scales are given respectively by $v_{edd}^2(k) \equiv 4\pi W(k)k^3 \propto k^{-2/3}$ and $\tau_{edd}(k) \equiv 2\pi/kv_{edd} = \pi^{1/2}(Wk^5)^{-1/2} \propto k^{-2/3}$, where $W(k) = (u^2/4\pi)(2\pi/L)^{2/3}k^{-11/3} = (4\pi)^{-1}(2\pi Q/C_1\rho)^{2/3}k^{-11/3} \propto k^{-11/3}$ is the isotropic turbulence power spectrum, $k = 2\pi/l$ is the wave number and l is the eddy size. From the three-dimensional Kolmogorov constant $C \simeq 1.62$ [10], we obtain $C_1 = 2\pi/C^{3/2} = 3.05$. At the turbulence generation scale $k_m = 2\pi/L$, $v_{edd} = u$, $Q = 2C_1\rho[4\pi W^3 k^{11}]^{1/2} = C_1\rho v_{edd}^2(k)/\tau_{edd}(k)$, and the total turbulence energy is given by $\int W(k)4\pi k^2 dk = (3/2)u^2$. The turbulence decay time is therefore given by $\tau_d = 3\tau_{edd}(k_m)/C_1$, i.e., eddies decay after making $3C_1^{-1} \sim 1$ turns.

We are interested in the acceleration of particles through scattering randomly with heavy scattering centers with the corresponding acceleration time $\tau_{ac} = \tau_{sc}[3v^2/v_{edd}^2(k)]$, where $\tau_{sc} = 2\pi/kv = l/v$ is the scattering time, v is the particle speed, and we have assumed that the scattering mean free-path is equal to l . For the above isotropic Kolmogorov turbulence spectrum, $\tau_{ac}(k) = 3v/2Wk^4 \propto k^{-1/3}$. To have significant stochastic particle acceleration (SA), the acceleration time $\tau_{ac}(k)$ should be shorter than the turbulence de-

cay time τ_d , which implies $u^2 > C_1 v v_{edd}(k)$. So, in general, the SA is more efficient at smaller scales. The onset scale of the SA is given by $k_c = (C_1 v/u)^3 k_m$. Therefore, to produce energetic particles with a speed of v by a Kolmogorov spectrum of scattering centers, the turbulence must have a dynamical range greater than $D_k = (C_1 v/u)^3$.

In the Kraichnan phenomenology, the turbulence decay is suppressed by the wave propagating effect with $Q = C_1 \rho u^4 / Lv_F$, $W(k) = (u^2/4\pi)k_m^{1/2}k^{-7/2}$, $\tau_{edd} \propto k^{-3/4}$, $v_{edd} \propto k^{-1/4}$, $\tau_{ac} \propto k^{-1/2}$, and the turbulence decay time $\tau_d = 3\tau_{edd}(k_m)v_F/C_1 u$, where the wave speed $v_F \gg u$. To have significant acceleration through scattering with the eddies, the dynamical range of the turbulence must be greater than $D_w = (C_1 v/v_F)^2$, which is much less than $D_k = (C_1 v/u)^3$. The resonant interactions of particles with waves can be much more efficient in accelerating particles in this case. For a wave speed v_F independent of k , the acceleration time is given by $\tau_{ac} = 3\tau_{sc}v^2/v_F^2 \propto k^{-1}$. To have significant acceleration, the scattering mean free path of the particles must be shorter than $(v_F^3/C_1 v u^2)L = D_k^{2/3}D_w^{-3/2}L$.

Several Shell-Type Supernova Remnants (STSNRs) have been observed extensively in the radio, X-ray, and TeV bands. X-ray observations with *Chandra*, *XMM-Newton*, and *Suzaku* and TeV observations with HESS have made several surprising discoveries that challenge the classical diffusive shock particle acceleration model [3, 8]. The SNR RX J1713.7-3946 is about $t = 1600$ years old [9] with a radius of $R \simeq 10$ pc and a distance of $D \simeq 1$ kpc. By fitting its broadband spectrum with an electron distribution of $f \propto \gamma^{-p} \exp(-\gamma/\gamma_c)^{1/2}$, we

find that $p = 1.85$, $B = 12.0 \mu\text{G}$, $\gamma_e m_e c^2 = 3.68 \text{ TeV}$, and the total energy of relativistic electrons with the Lorentz factor $\gamma > 1800 E_e = 3.92 \times 10^{47} \text{ erg}$ (Fig. 6).

The X-ray emitting electrons have a gyro-radius of $r_g \simeq 10^{15} \text{ cm}$, which shouldn't be shorter than the scattering mean free path. To produce these electrons through the SA, the turbulence must be generated on scales greater than $D_k r_g$, $D_w r_g$, and $D_w^{3/2} D_k^{-2/3} r_g$ for the non-resonance Kolmogorov, Kraichnan phenomenology, and the resonant interactions, respectively. For STSNRs, $u \sim v_F \sim 0.01c$, $D_k r_g \sim 10 \text{ kpc}$, which is much larger than the radii of the remnants. The SA by eddies with a Kolmogorov spectrum is therefore insignificant. $D_w r_g \sim 30 \text{ pc}$, which is also too thick. $D_w^{3/2} D_k^{-2/3} r_g \sim 0.1 \text{ pc}$, which is much greater than the particle inertial length and may be generated through the Kelvin-Helmholtz instabilities or cosmic ray drifting upstream [4, 5]. Therefore if relativistic electrons from the STSNRs are accelerated through the SA, they must be energized through resonant interactions with high speed plasma waves. Low speed waves also require a large turbulence dynamical range to accelerate particles.

SHOCK STRUCTURE, WAVE DAMPING, AND STOCHASTIC ELECTRON ACCELERATION BY FAST MODE WAVES IN THE DOWNSTREAM

We next study the SA in the shock downstream by weakly magnetized turbulence with the Alfvén speed $v_A = (B^2/4\pi\rho)^{1/2} \ll u$, where B , and ρ are the magnetic field, and mass density, respectively. For strong non-relativistic shocks with the shock frame upstream speed U much higher than the speed of the parallel propagating fast mode waves in the upstream $v_F = (v_A^2 + 5v_S^2/3)^{1/2}$, where $v_S^2 = P/\rho$ is the isothermal sound speed and P is the gas pressure, mass, momentum, and energy conservation across the shock front require

$$U^2 = 5v_S^2 + 5u^2 + 2v_A^2 + U^2/16, \quad (1)$$

where we have assumed that the turbulence behaves as an ideal gas and ignored the wave propagation effects. The shock structure can be complicated due to the present of turbulence. We assume that the turbulence is isotropic and has a generation scale of L , which does not change in the downstream. The speeds v_S , v_A , and u therefore should be considered as averaged quantities on the scale L . v_A depends on the upstream conditions and/or the dynamo process of magnetic field amplification[1, 5]. Here we assume it a constant in the downstream. One can then quantify the evolution of other speeds in the downstream.

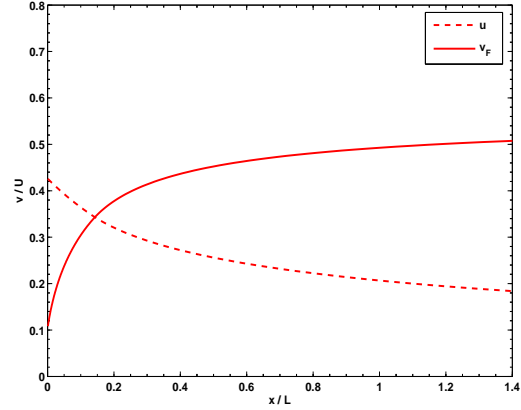


FIGURE 1. Evolution of the eddy speed u and speed of parallel propagating fast mode waves v_F in the downstream for $v_A = 0.0633U$.

For the Kolmogorov phenomenology,

$$\frac{3d\rho u^2}{2dt} = -Q \quad \text{i.e.,} \quad \frac{3Udu(x)^2}{8dx} = -\frac{C_1 u(x)^3}{L}. \quad (2)$$

Near the shock front, we denote the isothermal sound speed and Alfvén speed by v_{S0} and v_{A0} , respectively. Then the eddy speed at the shock front is given by $a^{1/2}U/4$ with $a = 3 - 16v_{S0}^2/U^2 - 32v_{A0}^2/5U^2$. Integrate equation (2) from the shock front ($x = 0$) to downstream ($x > 0$), we then have

$$\frac{u(x)}{U} = \frac{1}{4C_1 x/3L + 4/a^{1/2}}, \quad (3)$$

$$\frac{v_S(x)}{U} = \left[\frac{3}{16} - \frac{1}{16(C_1 x/3L + a^{-1/2})^2} - \frac{2v_A^2}{5U^2} \right]^{1/2} \quad (4)$$

$$\frac{v_F(x)}{U} = \left[\frac{5}{16} - \frac{5}{48(C_1 x/3L + a^{-1/2})^2} + \frac{v_A^2}{3U^2} \right]^{1/2} \quad (5)$$

As mentioned in the previous section, to produce the observed X-ray emitting electrons in the STSNRs through the SA processes, fast mode waves must be excited efficiently. The MHD wave period is given by $\tau_F(k) = 2\pi/v_F k$. Then the transition scale from the Kolmogorov to Kraichnan phenomenology occurs at $\tau_F(k_t) = \tau_{edd}(k_t)$ or $v_F = v_{edd}(k_t)$ [2]. We then have

$$k_t = (u/v_F)^3 k_m. \quad (6)$$

For $k > k_t > k_m$, the turbulence spectrum in the inertial range is given by $W(k) = u^2(4\pi)^{-1} k_m^{2/3} k_t^{-1/6} k^{-7/2} = (4\pi)^{-1} v_F^{1/2} u^{3/2} k_m^{1/2} k^{-7/2}$. Although the turbulence energy exceeds $(3/2)u^2$ when the wave propagation effect

is considered, we still assume that the enthalpy of the turbulence is given by $(5/2)u^2$ for $v_F < u$ so that equation (1) and the above solutions for the speed profiles remain valid.

In the subsonic phase with $v_F > u$, we assume that fast mode waves can still be excited efficiently to maximize the SA efficiency. Then the Kraichnan phenomenology prevails and

$$\begin{aligned} W(k) &= u^2(4\pi)^{-1}k_m^{1/2}k^{-7/2}, \quad (7) \\ \frac{3Udu(x)^2}{8dx} &= -\frac{C_1u(x)^4}{Lv_F} \quad (8) \end{aligned}$$

where from equation (1) one has $v_F = [5U^2/16 + v_A^2/3 - 5u^2(x)/3]^{1/2}$. These equations can be solved numerically to get the speed profiles in the subsonic phase. Figure 1 shows the v_F and u profiles with $v_A = v_{A0} = 0.0633U$ in the downstream and $v_{S0} = v_{A0} \ll U$.

In summary,

$$W(k) = u^{3/2}(4\pi)^{-1} \min(v_F^{1/2}, u^{1/2})k_m^{1/2}k^{-7/2} \quad (9)$$

in the Kraichnan regime. The collisionless damping starts at the coherent length of the magnetic field $l_d = 2\pi/k_d$, where the period of Alfvén waves $2\pi/kv_A$ is comparable to the eddy turnover time, i.e., $v_A^2 = 4\pi W(k_d)k_d^3 = \min(v_F^{1/2}, u^{1/2})u^{3/2}k_m^{1/2}k_d^{-1/2}$. Then we have

$$k_d = [u^3 \min(v_F, u)/v_A^4]k_m. \quad (10)$$

For a fully ionized hydrogen plasma with isotropic particle distributions, which is reasonable in the absence of strong large scale magnetic fields, the transit-time damping (TTD) rate is given by [7, 6]

$$\begin{aligned} \Lambda_T(\theta, k) &= \frac{(2\pi k_B)^{1/2}k \sin^2 \theta}{2(m_e + m_p) \cos \theta} \times \\ &\left[(T_e m_e)^{1/2} e^{-\frac{m_e \omega^2}{2k_B T_e k_{\parallel}^2}} + (T_p m_p)^{1/2} e^{-\frac{m_p \omega^2}{2k_B T_p k_{\parallel}^2}} \right] \quad (11) \end{aligned}$$

where k_B , T_e , T_p , m_e , m_p , θ , ω , and $k_{\parallel} = k \cos \theta$ are the Boltzmann constant, electron and proton temperatures, masses, angle between the wave propagation direction and mean magnetic field, wave frequency, and parallel component of the wave vector, respectively. The first and second terms in the brackets on the right hand side correspond to damping by electrons and protons, respectively. For weakly magnetized plasma with $v_A < v_S$, proton heating always dominates the TTD for $\omega^2/k_{\parallel}^2 \sim v_S^2 \sim k_B T_p/m_p$. If v_A does not change dramatically in the downstream, the continuous heating of background particles through the TTD processes makes $T_p \rightarrow (m_p/m_e)T_e$ since the heating rates are proportional

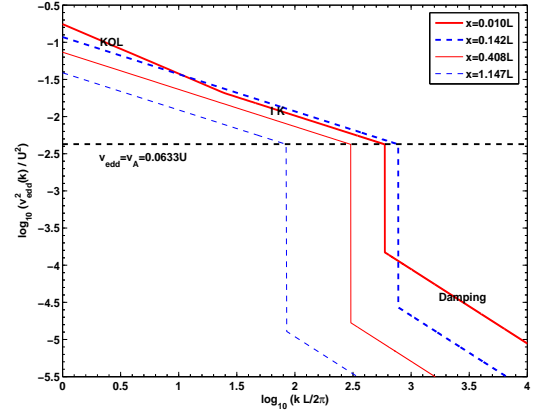


FIGURE 2. The turbulence spectra $v_{edd}^2(k)$ at several locations in the downstream as indicated. The Kolmogorov, Kraichnan, and damping ranges are indicated for the supersonic phase spectrum with $x = 0.010L$. At the other locations, the turbulence is subsonic and there are only Kraichnan and damping ranges. The sharp drops of the turbulence spectra in the damping range are due to the onset of thermal damping at the coherent length of the magnetic field $2\pi/k_d$.

to $(mT)^{1/2}$, where m and T represent the mass and temperature of the particles, respectively. We see that parallel propagating waves (with $\sin \theta = 0$) are not subject to the TTD processes and can accelerate some particles to very high energy through cyclotron resonances. Obliquely propagating waves are damped efficiently by the background particles. Although the damping rates for waves propagating nearly perpendicular to the magnetic field ($\cos \theta \simeq 0$) are also low, these waves are subject to damping by magnetic field wandering [6]. The turbulence power spectrum cuts off sharply when the damping rate becomes comparable to the turbulence cascade rate $\Gamma = \tau_{edd}^{-2}/(\tau_F^{-1} + \tau_{edd}^{-1}) \simeq \tau_{edd}^{-2} \tau_F$ [2]. One can define a critical propagation angle $\theta_c(k)$, where $\Lambda_T(\theta_c, k) = \Gamma(k)$. Equations (9) and (11) give

$$\frac{v_A^2 k_d^{1/2}}{2^{1/2} \pi^{3/2} v_S v_F k^{1/2}} \simeq \frac{\sin^2 \theta_c}{\cos \theta_c} \exp\left(-\frac{v_F^2}{2v_S^2 \cos^2 \theta_c}\right), \quad (12)$$

where the electron damping term has been ignored. The turbulence spectra at several locations in the downstream are shown in Figure 2.

The escape time of relativistic particles with $v \simeq c$, where c is the speed of light, from the particle acceleration region is given by $\tau_{esc} = (L^2/4c^2)\tau_{sc}$ and the spectral index of the accelerated particles in the steady state is given by

$$p = \left(\frac{9}{4} + \frac{\tau_{ac}}{\tau_{esc}}\right)^{1/2} - \frac{1}{2} = \left(\frac{9}{4} + \frac{12c^2 k_m^2}{v_F^2 k_d^2}\right)^{1/2} - \frac{1}{2}$$

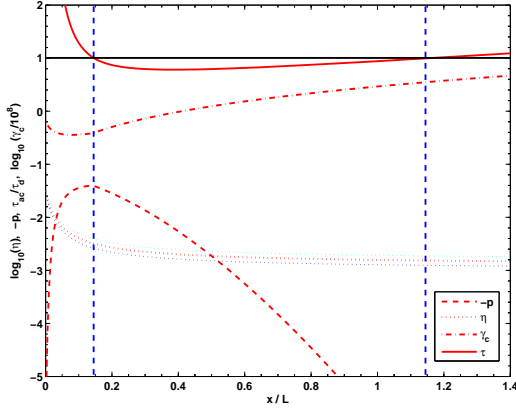


FIGURE 3. Evolution of the acceleration efficiency η (dotted), cutoff Lorentz factor γ_c (dotted-dashed), spectral index p (dashed), and $\tau = \tau_{ac}/\tau_d$ (solid) in the downstream for $v_A = 0.0633U$ and $U = 0.01c$. The particle acceleration is significant for $\tau < 1$, i.e., between the two vertical dashed lines indicating x_1 and x_2 . For γ_c , we have assumed that $B = 12\mu\text{G}$ and $L = 0.15\text{pc}$. For η , the two thin lines are for $U = 0.015c$ (higher) and $0.0067c$ (lower). See the following section for details

$$= \left[\frac{9}{4} + \frac{12c^2v_A^8}{u^6v_F^2 \min(v_F, u^2)} \right]^{1/2} - \frac{1}{2}. \quad (13)$$

We note that for v_A independent of x in the downstream, p reaches its minimum at the transonic point x_0 , where $v_F = u$. The maximum energy that particles can reach through resonant interactions with these parallel propagating waves is given by

$$\gamma_c = \frac{2\pi qB}{m_e c^2 k_d} = \frac{qBLv_A^4}{m_e c^2 u^3 \min(v_F, u)}, \quad (14)$$

where q is the elementary charge units. The ratio of the dissipated energy carried by non-thermal particles to that of the thermal particles should be greater than

$$\eta = \frac{\theta_c^2(k_d)}{4} = \frac{e^{5/6}v_A^2}{2(2\pi)^{3/2}v_S v_F} = \frac{e^{5/6}v_A^2}{2(2\pi)^{3/2}v_S v_F}, \quad (15)$$

where $e = 2.72$, since the isotropic turbulence with $k < k_d$ can also accelerate particles with the Lorentz factor $\gamma \geq \gamma_c$. To have efficient acceleration of relativistic particles, the turbulence decay time $\tau_d = 3 \max(u, v_F)L/C_1 u^2$ should be longer than the acceleration time $\tau_{ac} = (3c^2/v_F^2)\tau_{sc} = 6\pi c/v_F k_d = 3cv_A^4 L/v_F^2 u^3 \min(v_F, u)$, which implies $\max(u, v_F)L/C_1 u^2 > cv_A^4 L/v_F^2 u^3 \min(v_F, u)$, i.e., $C_1 < u^2 v_F^3 / cv_A^4$. There are at most two locations $x_1 < x_2$ in the downstream, where $\tau = \tau_{ac}/\tau_d = 1$ and $C_1 = u^2 v_F^3 / cv_A^4$. In combination with equation (13), significant particle acceleration occurs for

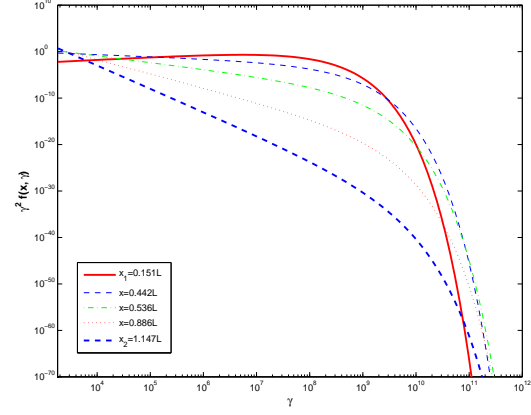


FIGURE 4. Normalized nonthermal electron distribution f produced at several locations in the downstream.

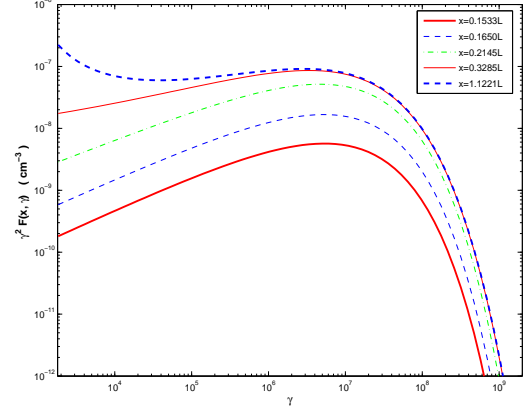


FIGURE 5. The distributions of nonthermal electrons F in the downstream.

$p < \left[\frac{9}{4} + 12v_F^2 \max(u^2, v_F^2) / u^4 C_1^2 \right]^{1/2} - 1/2$. The particle acceleration in the supersonic phase, i.e., $v_F < u$, therefore produces very hard electron distributions with $p < 1.39$ for $C_1 = 3$. Softer electron distributions have to be produced in the subsonic phase. Figure 3 shows the evolution of η , γ_c , p , and $\tau = \tau_{ac}/\tau_d$ in the downstream for $U = 0.01c$. The profiles of v_F/U and u/U only depend on v_A/U . So is the profile of η . τ and p also depend on the absolute value of U . To obtain γ_c , one needs to know L and B as well. In the extremely supersonic phase with $v_F \ll u$, the SA is negligible. The SA is significant only after the plasma is already heated up so that $v_F \sim u$. In the late subsonic phase, $u \ll v_F$, the SA is also insignificant since most of the free energy of the system has been converted into heat.

The particle distribution may be approximated reasonably well with $f(x, \gamma) \propto \gamma^{-p(x)} \exp -[\gamma/\gamma_c(x)]^{1/2}$ [3]. Then the distribution of non-thermal particle in the downstream

$$F(x, \gamma) = \int_{x_1}^x f(x', \gamma) \eta(x') (4Q/m_e c^2 U) dx' \quad (16)$$

where $\int_{m_p/m_e}^{\infty} \gamma f(x', \gamma) d\gamma = 1$, and $\int_{m_p/m_e}^{\infty} \gamma m_e c^2 F(x, \gamma) d\gamma$ gives the energy density of non-thermal particles at x . If $u^5/cv_A^4 < C_1$ at the sonic point x_0 , then $x_0 < x_1$ and there will be no particle acceleration in the supersonic phase. Figures 4 and 5 show the normalized electron distribution f and F at several locations in the downstream, respectively.

RESULTS

Here, we use the SNR RX J1713.7-3946 as an example to demonstrate how the SA by fast mode waves accounts for the observed broadband spectrum. Figure 6 shows the best fit with $v_A/U = 0.0633$, $L = 4.71 \times 10^{17}$ cm, $B = 12$ μ G and $U = 0.01c$. Comparing to the thin dashed line, which is derived by assuming an electron distribution $\propto \gamma^{-p} \exp -(\gamma/\gamma_c)^{1/2}$, there is a radio spectral bump due to electron acceleration relatively far from the shock front (see Figs. 4 and 5). In our model, there are five parameters: B , U , v_A , L , and the equivalent volume of a uniform emission range. The last is 4 times bigger than the volume of the SNR, suggesting higher nonthermal electron densities in the interior of the remnant than near the shock front. The observed radio to X-ray spectral index, X-ray to TeV flux ratio, location of the X-ray cutoff, and bolometric luminosity of the source give four constraints, which leads to one more degree of freedom. Our model fit to the spectrum therefore is not unique. However, B is uniquely determined by the ratio of the X-ray to TeV flux. To reproduce the observed spectral shape, the profiles of p , γ_c , and η should not change, which implies that $v_A^8 c^2 \propto u^{10}$ and $L \propto u^4/v_A^4$ at the transonic point x_0 . For $v_A \ll U$, u is proportional to U . We therefore obtain v_A and L as functions of U as indicated in Figure 7. The density can be derived from B and v_A , and the overall acceleration efficiency is defined as $\eta_{eq} = \int_{x_1}^{x_2} \eta Q dx / \int_0^{\infty} Q dx$. Nearly identical spectrum can be obtained for parameters on these lines. We note $\eta \propto v_A^2/v_{SVF} \propto v_A^2/U^2 \propto U^{1/2}$. The acceleration is more efficient in the earlier phase of the remnant evolution. The two thin dotted lines in Figure 3 show the dependence of η on U .

REFERENCES

1. Cho, J., & Vishniac, E. T. 2000, ApJ, 538, 217

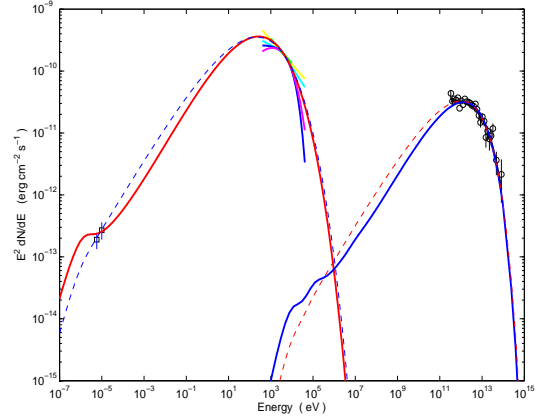


FIGURE 6. Best fits to the observed spectrum. The dashed line is for a simple power-law model with a gradual high energy cutoff. The solid line is for the fiducial model. The low and high energy spectral peaks are produced through the synchrotron and inverse Compton scattering of the background photons, respectively.

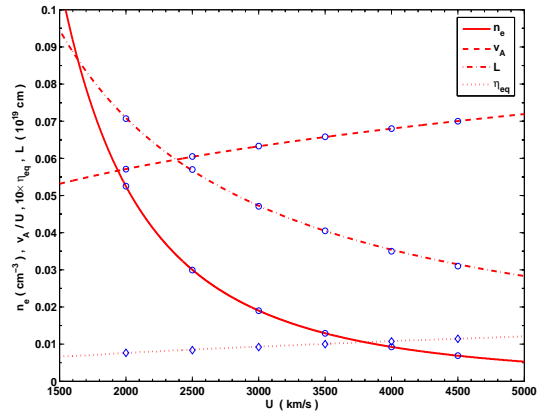


FIGURE 7. Nearly identical fit to the observations are obtained for parameters on these lines.

2. Jiang, Y. W., Liu, S. M., & Petrosian, V. 2008, astro-ph/0802.0910
3. Liu, S. M., Fan, Z. H., Fryer, C. L., Wang, J. M., & Li, H., 2008, ApJ, 683, L163
4. Micono, M., Zurlo, N., Massaglia, S., Ferrari, A., & Melrose, D. B. 1999, AA, 349, 323
5. Niemiec, J., Pohl, M., Stroman, T., & Nishikawa, K. I. 2008, ApJ, 684, 1171
6. Petrosian, V., Yan, H. R., & Lazarian, A. 2006, ApJ, 644, 603
7. Stix, T. H. 1962, The Theory of Plasma Waves (McGraw-Hill Book Company, inc.)
8. Takaaki, T., et al. 2008, ApJ, in press, astro-ph/0806.1490
9. Wang, Z. R., Qu, Q.-Y., & Chen, Y. 1997, A&A, 318L, 59
10. Yeung, P. K., & Zhou, Y. 1997, PhRvE, 56, 1746